Locally Controllable Manipulation by Stable Pushing

Kevin M. Lynch, *Member, IEEE*

***Abstract*—When a polygonal object is pushed with line contact along an edge, the push is called *stable* if the object remains fixed to the pusher. The object is *small-time locally controllable* by stable pushing if, by switching among pushing edges, it can be pushed to follow any path arbitrarily closely. Because the pushes are stable by the frictional mechanics, pushing plans can be executed without position feedback of the object. In this paper we derive a necessary and sufficient condition for a polygon to be small-time locally controllable by stable pushing: the pushing friction coefficient must be nonzero and the set of feasible pure forces (forces applied through a polygon edge and passing through the center of friction) must positively span the plane. We interpret this condition in terms of the polygon shape, the location of the center of friction, and the pushing friction coefficient, allowing us to characterize classes of polygons with this fundamental "maneuverability" property.**

***Index Terms*—Friction, robotic manipulation, small-time local controllability, stable pushing.**

I. Introduction and Motivation

PUSHING is a useful robot primitive for manipulating large, heavy, or slippery parts, parts with uncertain location, or parts that are otherwise difficult to grasp and carry. It can also simplify robot hardware by allowing the robot to push with any surface available (whole arm manipulation [1]) or by eliminating the need for a gripper in planar manipulation tasks. One application of pushing is parts feeding [2]–[6]. Pushing also allows a mobile robot to easily manipulate large objects [7], [8].

We are interested in characterizing the fundamental capabilities of pushing as a manipulation primitive. Toward that end we have studied the *controllability* of pushing: is it possible to push the object to the goal configuration? We distinguish between the following two versions of controllability:

1) Controllability: The object is *controllable* if it can be pushed from any configuration (position and orientation) to any other configuration in the obstacle-free three-dimensional (3-D) planar configuration space $SE(2) = \Re^2 \times S^1$. This is a global concept—the object may have to be pushed far away to reach a nearby configuration. Similarly, a car with no reverse gear is controllable on $SE(2)$, but it must travel a long distance forward (and turning) to accomplish a small back-up motion.

2) Small-Time Local Controllability: The object is *small-time locally controllable* on its entire configuration space $SE(2)$ if, for any configuration $\mathbf{q} \in SE(2)$ and any neighborhood U of $\mathbf{q}$, the set of configurations the object can reach without leaving U is a neighborhood of $\mathbf{q}$.[1] By patching together neighborhoods, the object can be pushed to follow any path arbitrarily closely, and therefore can be maneuvered in tight spaces. This is a stronger condition than controllability. A car which can reverse is small-time locally controllable, as evidenced by the ability to parallel park.

Other versions of nonlinear controllability are described by Sussmann [9]. In this paper we are interested in small-time local controllability.

We have previously shown that almost any object is small-time locally controllable by pushing with point contact [10]. This result implies that a two-degrees-of-freedom robot (a point translating in the plane) can maneuver an object to follow any path in its 3-D configuration space $SE(2)$ arbitrarily closely. The only exception is a disk centered at its center of friction with zero friction at the pushing contact—no torques can be generated about the center of friction, and the object cannot be rotated.

Pushing with point contact results in unpredictable motion of the object, making planning difficult. For this reason, we have also studied *stable pushing* with line contact between the object and the pusher [10], [11]. A stable push is defined as a pusher contact and motion that keeps the object fixed to the pusher as it moves. The pushing contact is mechanically stabilized by the frictional forces acting on the object due to sliding on the support plane, allowing the push to be executed robustly without position feedback of the object. Stable pushes make it possible to plan pushing paths (Fig. 1). A pushing planner and experiments with an Adept robot are described in [10].

By switching the line contacts, as in Fig. 1, it is sometimes possible to achieve small-time local controllability by stable pushing. In this paper we derive a necessary and sufficient condition for small-time local controllability by stable pushing: the pushing friction coefficient must be nonzero and the set of feasible pure forces (forces applied through a polygon edge and passing through the center of friction) must positively span the plane. We interpret this condition in terms of the polygon shape, the location of the center of friction, and the pushing friction coefficient.

Consider the problem of positioning and orienting the key in Fig. 2 by pushing. If the key is small-time locally controllable by stable pushing, the robot can push the key to the goal configuration in a confined workspace without

Manuscript received September 27, 1996; revised December 14, 1998. This work was presented in part at the 1997 IEEE International Conference on Robotics and Automation, Albuquerque, NM. This paper was recommended for publication by Associate Editor R. Howe and Editor A. Goldenberg upon evaluation of the reviewers' comments.

The author is with the Mechanical Engineering Department, Northwestern University, Evanston, IL 60208 USA.

Publisher Item Identifier S 1042-296X(99)03382-0.

[1] The usual definition of small-time local controllability also requires the reachable set to be a neighborhood of the initial configuration for small elapsed time. In this paper we are not concerned with time, such as the time required to change pushing contacts, but we retain the standard term.

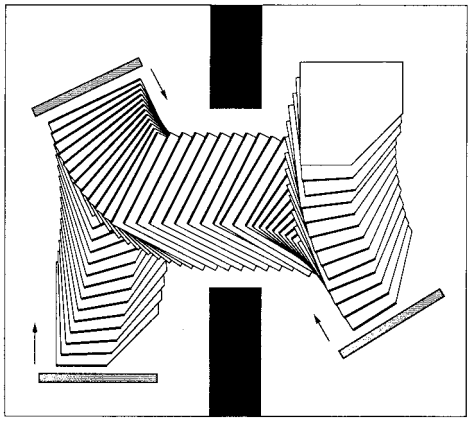

Fig. 1. Maneuvering a pentagon by stable pushing with line contact. This pentagon is small-time locally controllable using just the two pushing edges shown.

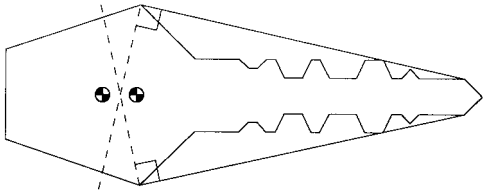

Fig. 2. A key and its polygonal convex hull. The line pusher can push on any edge of the convex hull. If the center of friction of the key is at the left position, a friction coefficient of at least 0.18 is required between the pusher and the key for small-time local controllability by stable pushing. If the center of friction is at the right, the key is small-time locally controllable for any nonzero friction coefficient. The design with the center of friction at the right is a preferable design for maneuvering the key with low contact friction.

position feedback of the key during execution. We can design the key to be small-time locally controllable by choosing its shape and center of friction. This is a simple type of *design for parts feeding.*

By considering geometry (the shape of the polygon) and the frictional mechanics of pushing, we can demonstrate this fundamental "maneuverability" property for classes of parts by stable pushing. One aim of the science of robotic manipulation is to elucidate such characterizations of manipulation primitives. Other related results in manipulation include the demonstration of the controllability of a ball rolling on a plane or another ball [12]; bounds on the number of fingers necessary for a grasp [13]–[15]; the classification of orientable parts by sensorless parallel-jaw grasping sequences [5]; and the proof that a one-joint robot operating above a fixed-speed conveyor is sufficient to position and orient polygonal parts by pushing [6]. Our work on characterizing controllable polygons in terms of their geometry is similar in spirit to the work of van der Stappen *et al.* [16] on characterizing the complexity of parts orienting in terms of the *geometric eccentricity* ("thinness") of the part.

We begin with a review of related work. In Section III we provide definitions and derive the necessary and sufficient condition used throughout the paper. Section IV gives an algorithm for finding the minimum pushing friction coefficient that yields small-time local controllability for a given part. Section V presents results on the minimum friction needed for small-time local controllability for classes of polygons. Proofs of these results are given in Section VI.

II. Related Work

In [10], we demonstrated that for any polygon there exists an edge from which it is controllable by stable pushes if the pushing friction coefficient is nonzero. In other words, any polygon can be moved to any configuration in an obstacle-free plane by stable pushing from a single edge. We also stated a sufficient condition for small-time local controllability when the pusher is allowed to switch pushing edges. This paper extends that work by providing a necessary and sufficient condition for polygons and interpreting it in terms of the part's shape, center of friction, and the pushing friction coefficient.

Our work builds on previous work on the mechanics of pushing. Mason [17] identified pushing as an important manipulation primitive and implemented a numerical routine to find the motion of an object with a known support distribution being pushed at a single point of contact. Recognizing that the support distribution is usually unknown and possibly varying, Mason derived a simple rule for determining the rotation sense of the pushed object that depends only on the location of the center of friction of the object. Mason and Brost [18] and Peshkin and Sanderson [19] followed this work by finding bounds on the rotation rate of the pushed object. These results were used to derive the stable pushing primitive [11]. Goyal, Ruina, and Papadopoulos [20], [21] developed a *limit surface* characterization of the relationship between the motion of the sliding object and the associated sliding friction forces when the object's support distribution is completely specified. Alexander and Maddocks [22] considered the other extreme, when only the geometric extent of the support area is known, and described techniques to bound the possible motions of the pushed object.

In this paper we assume that only the center of friction of the object is known. More information is unavailable since the distribution of support forces is generally indeterminate, and less information is often too weak for effective manipulation planning.

The controllability of a pushed object is closely related to the controllability of a nonholonomic mobile robot, which shares the same planar configuration space $SE(2)$. Small-time local controllability of a mobile robot results from its ability to reverse directions; for a pushed object, it results from changing pushing edges. If an object is small-time locally controllable by stable pushing, we can adapt path planning algorithms for mobile robots to find pushing plans [23], [24].

III. Definitions

The straight-edge robot pusher is called the *pusher* and the pushed object is called the *slider*. The slider is pushed across a horizontal support plane. We assume that the slider's motion is sufficiently slow that inertial forces are negligible compared to sliding friction. This is the *quasistatic* assumption. The state of the slider is simply its configuration $\mathbf{q} \in SE(2)$.

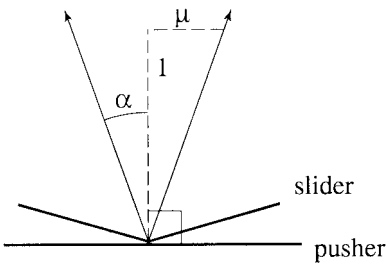

Fig. 3. Friction cone at a pushing contact. The half-angle of the friction cone is $\alpha = \tan^{-1}\mu$.

We study stable pushing with line contact. The slider is a convex polygon and the pusher is a flat edge aligned with an edge of the polygon. Because the pusher is a line, nonconvex polygons are equivalent to their convex hulls. The pusher can push on any edge of the slider's convex hull.

Friction between the pusher and the slider and between the slider and the support surface is assumed to conform to Coulomb's law. At a contact, the *friction angle* α is the half-angle of the cone of forces which can be applied through the contact. The *friction coefficient* μ is defined $\mu = \tan\alpha$. In this paper α and μ refer to friction at the contact between the pusher and the slider (Fig. 3).

The slider's *center of friction* $\mathbf{x}_c$ is given by

$$\mathbf{x}_c = \frac{\int_R \mathbf{x}\mu_s(\mathbf{x})p(\mathbf{x})\,dA}{\int_R \mu_s(\mathbf{x})p(\mathbf{x})\,dA} \tag{1}$$

where R is the support region of the slider, $\mu_s(\mathbf{x})$ is the support friction coefficient at the point $\mathbf{x} \in R$, $p(\mathbf{x})$ is the support pressure, and dA is a differential element of area of R. Because $\mu_s(\mathbf{x})$ and $p(\mathbf{x})$ are nonnegative, the center of friction cannot lie outside the convex hull of R. We assume that $\mu_s(\mathbf{x})p(\mathbf{x})$ is finite at all $\mathbf{x} \in R$, and therefore the center of friction lies in the *interior* of the convex hull of the slider. If the support friction coefficient $\mu_s(\mathbf{x})$ is uniform over R, then the $\mu_s(\mathbf{x})$ terms can be factored out of the integrals and canceled in (1). The resulting equation shows that the planar location of the center of friction is equivalent to that of the center of mass.

In this paper we assume that only the center of friction of the slider is known; no other information about $\mu_s(\mathbf{x})$ or $p(\mathbf{x})$ is available.

The frictional contact forces which can be applied through an edge form a polyhedral convex cone in the 3-D force-moment (*wrench* or *generalized force*) space measured in a body-fixed frame Σ_b affixed to the slider's center of friction (Fig. 4). This wrench cone is the convex hull of the forces and moments from the friction cones at each end of the edge. A force is in the *interior* of the wrench cone if it passes through the interior of the edge at an angle less than the friction angle α. A force is on the *boundary* of the wrench cone if it acts at the friction angle α or passes through an endpoint of the edge. A *pure force* is a contact force through the center of friction of the slider, yielding zero moment. We refer to *interior pure forces*, forces which are both interior and pure, and *boundary pure forces*, forces which are both on the boundary and pure. For any contact edge, the set of pure forces that can be applied is either empty, a single force direction (necessarily a boundary force), or a range of force directions (including a range of interior pure forces). The pure forces that can be applied through an edge are simply those forces that lie on or inside the friction cone and pass through both the edge and the center of friction (see Fig. 5).

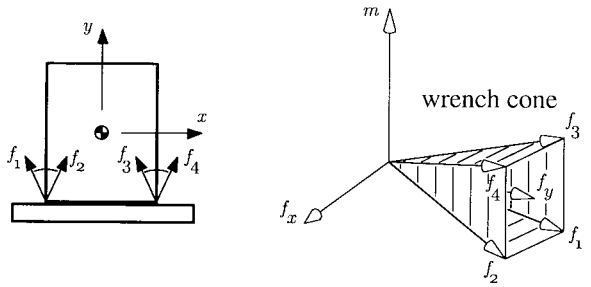

Fig. 4. Contact forces through an edge are the convex combination of the friction cones at each end of the edge. These friction forces can be represented as a convex cone in the slider's 3-D force-moment space [25], [26]. Boundary forces (through an edge endpoint or at a friction boundary) are the outer "shell" and interior forces are all forces inside the shell. Forces in the $m = 0$ plane are pure forces.

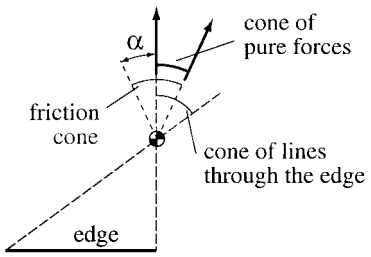

Fig. 5. The cone of pure forces that can be applied through an edge is the intersection of the friction cone drawn at the center of friction and the cone formed by lines through the center of friction and the two endpoints of the edge. The boundary pure forces are the boundaries of the cone.

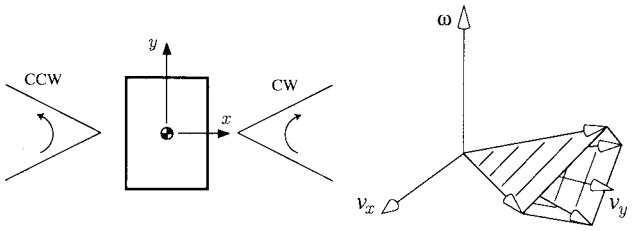

Fig. 6. The same set of velocities represented as clockwise and counterclockwise rotation centers and as a cone in the velocity space. Note that the CCW and CW rotation center regions actually meet at infinity (which corresponds to translations), forming a single connected region, just as with the velocity cone. Boundary velocities correspond to the edges of the rotation center region and the boundary of the velocity cone.

The velocity of the slider can be represented either as a rotation center or as a point in the 3-D (v_x, v_y, ω) (*twist* or *generalized velocity*) space, also measured in the body-fixed frame Σ_b. The rotation center is the point in the plane about which every point of the slider is instantaneously rotating. (This point is at infinity if the slider is moving without rotation.) The rotation center for a velocity (v_x, v_y, ω) is

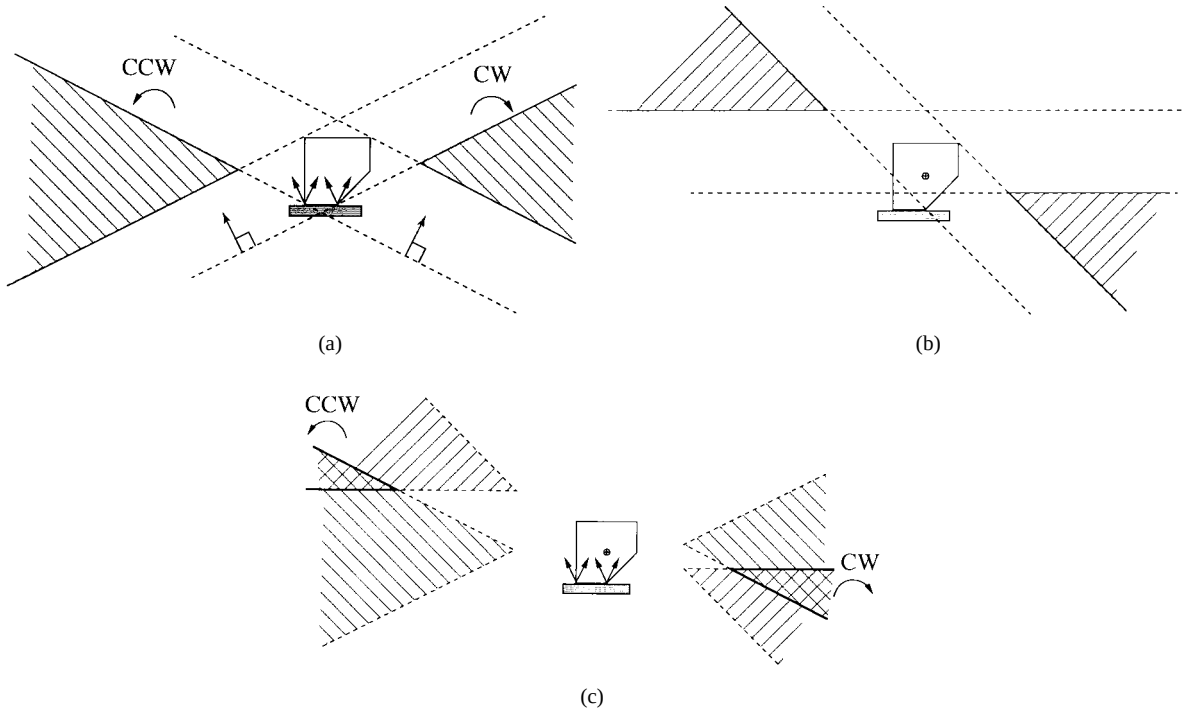

Fig. 7. (a) Coefficient of friction (0.5 here) defines the left and right edges of the friction cone. For each edge of the friction cone, draw two lines perpendicular to the friction cone edge such that the entire slider is contained between the two lines. The area between these two lines defines a band associated with the friction cone edge. Any contact force along a friction cone edge, regardless of the point of application, will result in a rotation center in that edge's band. Counterclockwise (clockwise) rotation centers which lie to the left (right) of the slider and between the two bands correspond to forces inside the angular limits of the friction cone. (b) For each endpoint of the line contact, draw two lines perpendicular to the line through the endpoint and the center of friction. One of these lines is the perpendicular bisector between the contact point and the center of friction. The other is a distance r^2/p from the center of friction and on the opposite side from the endpoint, where p is the distance from the endpoint to the center of friction and r is the distance from the center of friction to the most distant support point of the slider. (This "tip line" should actually be slightly more distant from the center of friction; see (Peshkin and Sanderson [19]) for details.) The rotation center from pushing on this endpoint must lie in the band between these two lines. All rotation centers between the two bands correspond to forces that pass between the two endpoints. (c) The intersection of the closed regions found in (a) and (b) yield a set of rotation centers corresponding to forces that are guaranteed to lie on or inside the convex cone of forces from the line pushing contact. These rotation centers may also be expressed as a polyhedral convex cone of velocities in the slider's velocity space (v_x, v_y, ω).

at $(-v_y/\omega, v_x/\omega)$ in Σ_b. Rotation centers are convenient for graphical purposes, but the 3-D velocity space is more convenient for proofs. A *translation* is a velocity with a zero angular component. A set of velocities can be represented as a region of rotation centers or as a cone in the (v_x, v_y, ω) space. As with forces, we can define interior and boundary velocities of a set of velocities (Fig. 6).

A sufficient condition for small-time local controllability of a system at a state $\mathbf{q}$ is that the set of feasible motion directions (tangent vectors) positively spans the system's tangent space at $\mathbf{q}$ [27]. (Recall that a set of vectors $\mathcal{V}$ positively spans $\Re^n$ if and only if the convex hull of $\mathcal{V}$ contains the origin of $\Re^n$ in its interior.) For the slider, the tangent space is the 3-D space (v_x, v_y, ω) of slider velocities, and the tangent vectors are the stable pushing directions. If the stable pushing directions positively span the 3-D velocity space, the slider is small-time locally controllable by stable pushes.

In [10] we described the procedure STABLE that determines a set of stable pushing motions for a given line contact, friction coefficient, center of friction, and slider geometry. This procedure builds on results for point contact pushing derived by Mason and Brost [18] and Peshkin and Sanderson [19]. STABLE is described and illustrated in Fig. 7. The pushes found by STABLE are guaranteed to be stable for the known center of friction *regardless* of the slider's exact support distribution. We will use the following key properties of STABLE:

1) If an interior pure force can be applied through the edge, then STABLE finds a set of stable pushing directions with nonempty interior, including a range of translation directions aligned with the pure force directions. The stable pushing directions in the slider's velocity space form a polyhedral convex cone which lies partially above and partially below the $\omega = 0$ plane.
2) If a single pure force can be applied, STABLE finds a single translation direction aligned with the force. No other stable pushing motion can be found without more information about the slider's support distribution.
3) If no pure force can be applied through the edge, then STABLE finds no stable pushing motions, and it is impossible to identify any stable pushing motions without more information about the slider's support distribution.

Using these properties of STABLE, we can state the basis of the results derived in this paper.

Proposition 1: The convex polygonal slider is small-time locally controllable by stable pushes found by STABLE if and only if the pushing friction coefficient μ is nonzero and

boundary pure forces from the edge contacts positively span the plane.

Proof: Every slider has at least one edge from which a set of pure forces with nonempty interior can be applied, provided the friction coefficient μ is greater than zero. To find such an edge, draw the maximal inscribed circle centered at the center of friction. This circle contacts an interior point of at least one edge E. The normal to E at the contact point represents a pure force, and because this point is interior to E and $\mu > 0$, this normal corresponds to an interior pure force. Therefore a range of pure forces $\mathcal{F}_E^{pure}$ with nonempty interior can be applied through E. STABLE finds a cone of velocity directions $\mathcal{V}_E$ (with nonempty interior in the 3-D velocity space) with a set of translations $\mathcal{V}_E^{trans}$ aligned with $\mathcal{F}_E^{pure}$.

For every pure force applied from every other edge, STABLE finds a translational velocity aligned with the force. The union of the boundary translations from these other edges is denoted $\mathcal{V}_{other}^{trans}$. If $\mathcal{V}_{other}^{trans}$ and $\mathcal{V}_E^{trans}$ positively span the plane, then $\mathcal{V}_{other}^{trans}$ and $\mathcal{V}_E$ positively span the space of slider velocities and the slider is small-time locally controllable. This is because $\mathcal{V}_E$ contains velocity directions with $\omega > 0$ and $\omega < 0$, and any two such velocity directions, plus a set of velocity directions positively spanning the $\omega = 0$ plane, positively span the 3-D velocity space.

This proves that the conditions of the proposition are sufficient. To see they are necessary, assume the boundary pure forces positively span a half-plane. Then STABLE finds a set of velocity directions confined to an open half-space $\mathcal{H}$, along with two opposing translations on the plane bounding $\mathcal{H}$. These velocities do not yield small-time local controllability [10].

Finally note that if $\mu = 0$, STABLE finds only translational motions, and the slider cannot be rotated by pushes found by STABLE. (Such a slider can certainly be rotated by pushing, but its motion depends on the exact form of the support distribution and is unpredictable.) □

Proposition 1 gives a simple way to determine if a given convex polygonal slider is small-time locally controllable by pushes found by STABLE for a given friction coefficient $\mu > 0$: simply construct the boundary pure forces for each edge and check if they positively span the plane. Fig. 8 shows the pure forces for the key in Fig. 2 with $\mu = 0.1$ and the two different locations of the center of friction. Proposition 1 shows that one of the keys is small-time locally controllable while the other is not.

IV. MINIMUM FRICTION ALGORITHM

Given a particular slider we would like to find the minimum friction coefficient μ that makes it small-time locally controllable by pushes found by STABLE. Such a friction coefficient always exists. As we increase the friction coefficient from zero, the cone of pure forces that can be applied from each edge increases (or remains unchanged) until we hit a critical friction coefficient at which the pure forces positively span the plane. Specifically, as the friction coefficient is increased from zero, the cone of pure forces which can be applied from an edge

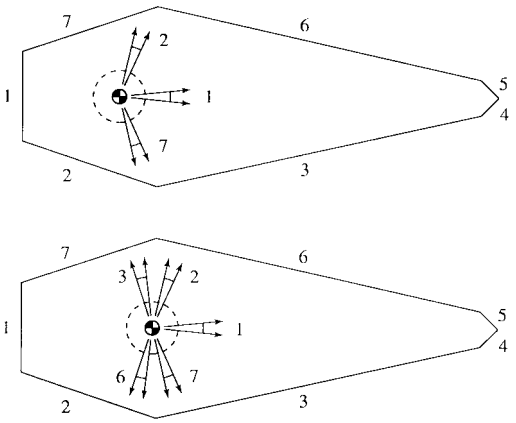

Fig. 8. Slider of Fig. 2 with $\mu = 0.1$ and the two different locations of the center of friction. Each edge is labeled, and the pure forces which can be applied through each edge are shown. Top: Pure forces can only be applied through edges 1, 2, and 7, and they do not positively span the plane. The slider is not small-time locally controllable by stable pushing. The shaded portion of the (x, y) ball around the center of friction shows the positions the center of friction can reach by stable pushing without leaving the ball. Bottom: Pure forces can be applied through edges 1, 2, 3, 6, and 7, and these forces positively span the plane. The slider is small-time locally controllable, and the center of friction can reach any position inside the open ball without leaving the ball. In fact, this slider is small-time locally controllable using only edges 2 and 6 or 3 and 7.

(Fig. 5) passes through stages 2 and 3 or stages 1–3 of the following three-stage sequence:

1) No pure forces can be applied from the edge.
2) The cone of pure forces increases monotonically with the friction coefficient.
3) The cone of pure forces remains unchanged as the friction coefficient is increased. The edge geometry determines the maximum cone of pure forces.

This observation allows us to derive the following algorithm to identify the minimum friction coefficient which yields small-time local controllability.

A. Minimum Friction Algorithm

1) Find the set of all critical friction angles at which the slider might become small-time locally controllable. These critical friction angles are illustrated in Fig. 9. A Type 1 critical friction angle is the minimum friction angle at which a pure force can be applied through an edge. A Type 2 critical friction angle is the minimum friction angle at which opposing pure forces can be applied through a pair of edges. (Opposing pure forces cannot be applied through some pairs of edges regardless of the friction angle. This occurs if there is no line through the center of friction that intersects both edges.) The set of all critical friction angles consists of the Type 1 angles for each edge and the Type 2 angles for each pair of edges. The set of pure forces can only transition to positively spanning the plane at one of these critical friction angles.
2) Sort the corresponding friction coefficients $\mu = \tan \alpha$ in increasing order. Each friction coefficient should retain its type information. Remove duplicates. If there are

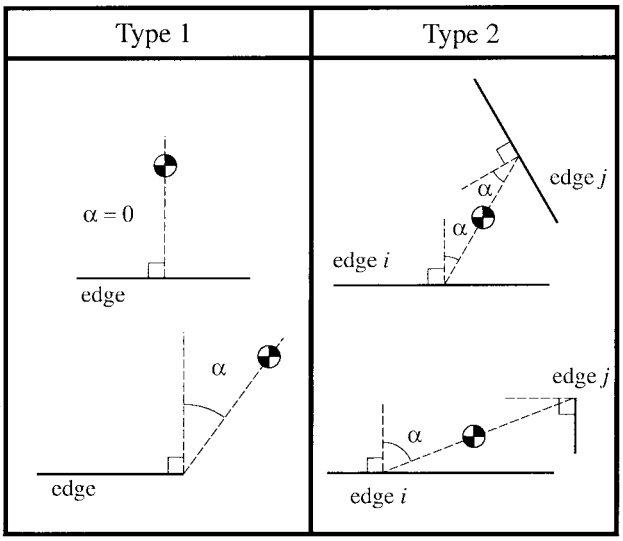

Fig. 9. Critical friction angles. Type 1: For each edge, the critical friction angle α is the minimum friction angle such that a force through the center of friction can be applied through the edge. Type 2: For each pair of edges, the critical friction angle α is the minimum friction angle needed for opposing pure forces to be applied through the edges. Opposing pure forces cannot be applied through some pairs of edges regardless of the friction angle. This occurs if there is no line through the center of friction that intersects both edges.

Type 1 and 2 friction coefficients with the same friction value, discard the Type 2 friction coefficient.

3) Evaluate the increasing friction coefficients until one is found which yields small-time local controllability.

Step 2 yields a sorted list of friction coefficients $(\mu_1, \mu_2, \cdots, \mu_n)$, where $\mu_1 = 0$. To evaluate μ_i in step 3, we actually evaluate $\mu_i + \delta$, where $\delta > 0$ and $\mu_i + \delta < \mu_{i+1}$. If the boundary pure forces positively span the plane for $\mu_i + \delta$, then the slider is small-time locally controllable for any friction coefficient $\mu > \mu_i$, since the transition could only have occurred at μ_i. If the critical friction coefficient $\mu_i > 0$ is of Type 1 and the boundary pure forces also positively span the plane for μ_i, the slider is small-time locally controllable for any $\mu \geq \mu_i$. This is because a Type 1 friction coefficient μ_i introduces a pure force from a new edge which may cause the pure forces to positively span the plane at exactly $\mu = \mu_i$. A Type 2 friction coefficient μ_i merely implies that boundary pure forces positively span a *line* at μ_i, which may expand to a plane for $\mu > \mu_i$. Examples are shown in Fig. 10.

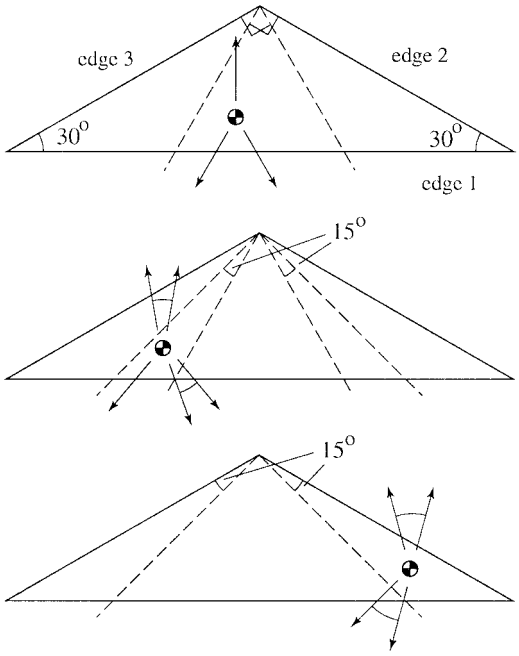

Fig. 10. Minimum friction algorithm applied to an isosceles triangle. Top: For any center of friction in the shaded region, each edge can apply a pure force at $\mu = 0$. These pure forces positively span the plane, and the slider is small-time locally controllable for any $\mu > 0$. Middle: For any center of friction in the shaded regions, the slider becomes small-time locally controllable at the minimum friction coefficient such that all edges can apply a pure force. For the center of friction shown, edge 2 can apply a pure force at $\mu \geq \tan 10^\circ \approx 0.176$. This is a Type 1 critical friction coefficient, and since the pure forces positively span the plane at $\mu = \tan 10^\circ$, the slider is small-time locally controllable for any $\mu \geq \tan 10^\circ$. Bottom: For any center of friction in the shaded regions, the slider becomes small-time locally controllable at the critical friction coefficient such that edges 1 and 2 or edges 1 and 3 can apply opposing pure forces. This occurs when $\mu = \tan 15^\circ \approx 0.268$, as shown in the figure. Note that this is a Type 2 critical friction coefficient; the pure forces do not positively span a plane at $\mu = \tan 15^\circ$. The slider is small-time locally controllable for $\mu > \tan 15^\circ$.

TABLE I
WORST-CASE FRICTION COEFFICIENT μ_w FOR SMALL-TIME LOCAL CONTROLLABILITY FOR REGULAR k-GONS WHERE k IS ODD (THEOREM 1)

Edges (k)	Friction (μ_w)
5	0.325
7	0.228
9	0.176
11	0.144
13	0.121

V. CLASSES OF LOCALLY CONTROLLABLE POLYGONS

Using Proposition 1 we can characterize classes of small-time locally controllable polygons based on their geometry, center of friction location, and contact friction. The proofs are given in Section VI.

Theorem 1 (Special Cases): The convex polygonal slider is small-time locally controllable by stable pushing with line contact, regardless of the location of the center of friction, if

1) $\mu > 0$ and the slider is a rectangle, a regular $2k$-gon ($k \geq 3$), or a triangle with all interior angles less than or equal to $\pi/2$, or

2) $\mu \geq \tan(\pi/2k)$ and the slider is a regular k-gon (k is odd, $k \geq 5$).

Theorem 2 (Number of Edges): Any convex k-gon slider is small-time locally controllable by stable pushing with line contact, regardless of the location of the center of friction, if $\mu \geq \tan(\pi/2 - \pi/k)$.

Theorem 2 implies that there exists a finite friction coefficient that yields small-time local controllability for any convex polygon. Some worst-case friction coefficients for regular k-gons (Theorem 1) and arbitrary k-gons (Theorem 2) are given in Tables I and II.

TABLE II
WORST-CASE FRICTION COEFFICIENTS μ_w FOR SMALL-TIME LOCAL CONTROLLABILITY FOR ARBITRARY k-GONS (THEOREM 2)

Edges (k)	Friction (μ_w)
3	0.577
4	1.0
5	1.376
6	1.732
7	2.077

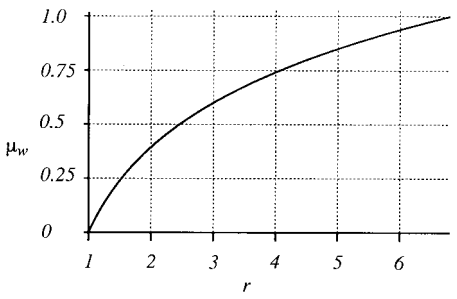

Fig. 11. Plot of the worst-case friction coefficients μ_w for small-time local controllability as a function of the ratio r of the radius of the minimal circumscribed circle to the radius of the maximal inscribed circle (Theorem 3). The region above the curve corresponds to polygons which are guaranteed to be small-time locally controllable by stable pushing.

The worst-case friction coefficients in Theorem 2 and part 2 of Theorem 1 require placing the slider's center of friction near a corner of the convex polygon, far from the geometric center of the slider. Thus another useful characterization of polygons is based on the location of the center of friction.

Theorem 3 (Center of Friction Location): Draw the largest inscribed circle and smallest circumscribed circle centered at the center of friction. The radius of the inscribed circle is a and the radius of the circumscribed circle is ra ($r > 1$). Then the ratio r and the worst-case friction angle α_w required for small-time local controllability are related by $r = f(\alpha_w) = \sec(\alpha_w)e^{(\pi/2)\tan\alpha_w}$. If $\mu \geq \tan\alpha_w = \tan f^{-1}(r)$ for the ratio r defined by the slider, the slider is small-time locally controllable by stable pushing with line contact.

Fig. 11 shows the curve of worst-case friction coefficients as a function of the ratio r, which can be thought of as the eccentricity of the part. Fig. 12 illustrates Theorem 3 for the case $r = 2$.

VI. PROOFS

Edges of a k-gon slider are numbered $1 \cdots k$ in a counterclockwise fashion. Vertices are also numbered $1 \cdots k$ counterclockwise such that edge 1 is bounded by vertices 1 and 2 and edge k is bounded by vertices k and 1. The interior angle between two adjacent edges is defined as in Fig. 13.

A. Theorem 1

1) If the slider is a rectangle or a triangle with all interior angles less than or equal to $\pi/2$, then the perpendicular projection of each edge contains the entire interior of the slider. Therefore each edge can apply a pure force through the center of friction, and these pure forces positively span the plane. If the friction coefficient μ is nonzero, then the slider is small-time locally controllable by Proposition 1.

   For a regular $2k$-gon, $k \geq 3$, there are always two opposing edges with opposing interior normals that pass through the center of friction regardless of its location. If $\mu > 0$, then pure forces from these two edges positively span the plane, and the slider is small-time locally controllable from these two edges. To find two such edges, draw the largest inscribed circle centered at the center of friction. Any edge that contacts the circle, along with its opposing edge, are sufficient for small-time local controllability.

2) A regular k-gon slider (k is odd, $k \geq 5$) is small-time locally controllable for any $\mu > 0$ and center of friction placement other than in one of $2k$ triangular regions near the vertices of the k-gon. Without loss of generality, consider the triangular regions R illustrated in Fig. 14. For a center of friction in R, only normals to edge 1 and edge $(k+1)/2$ pass through the center of friction. Since these edges are not opposite, they are not sufficient for small-time local controllability for all $\mu > 0$. Increasing the friction coefficient, the slider is guaranteed to be small-time locally controllable when the possible forces from edge $(k+3)/2$ cover the entire region R, i.e., a pure force can be applied through edge $(k+3)/2$ for any center of friction location in R. To find the required friction angle, draw the line segment C connecting vertex 1 and vertex $(k+5)/2$ (Fig. 15). The friction angle is the angle of C relative to the normals of

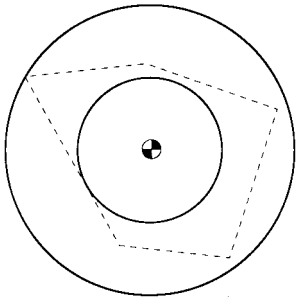

Fig. 12. Any polygon with its center of friction at the point indicated and a boundary outside the inner circle and inside the outer circle ($r = 2$) is small-time locally controllable by stable pushes for a friction coefficient $\mu \geq 0.395$. An example polygon is shown (see Theorem 3).

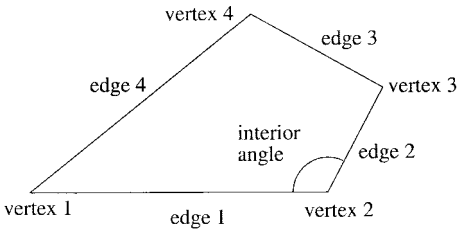

Fig. 13. Polygon definitions.

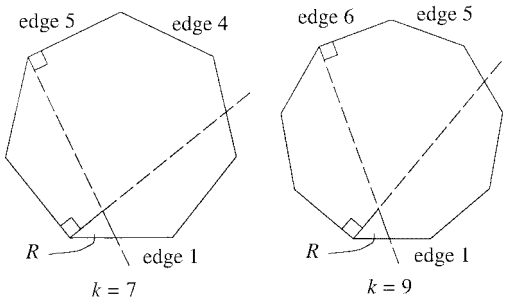

Fig. 14. Region R and its construction.

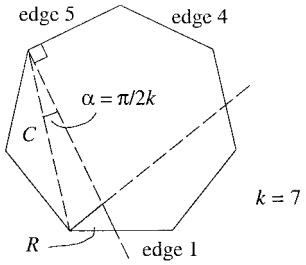

Fig. 15. Determining the worst-case friction angle required for small-time local controllability for a regular k-gon (k is odd, $k \geq 5$).

the two edges, $\pi/2k$. At this friction angle, pure forces from edges 1, $(k+1)/2$, and $(k+3)/2$ positively span the plane for any center of friction location in R. At any smaller friction angle, it is possible to choose a center of friction in R such that the pure forces do not positively span the plane.

B. Theorem 2

Assume the center of friction of the slider is at $(-\epsilon, \epsilon)$ ($\epsilon > 0$) and edge 1 of the slider is aligned with the x axis, stretching from $(-\infty, 0)$ to (0, 0). Edge 2 is at an interior angle of $\pi - 2\pi/k$ with respect to edge 1 and has length d. Edge n, $n = 3 \cdots k$, is at an angle $\pi - \pi/k$ with respect to edge $n-1$ with length d^{n-1} (except edge k, which has infinite length; see Fig. 16). Edge 1 and edge k are parallel and meet at infinity with zero interior angle. To be an actual polygon, of course, these edges cannot be exactly parallel, but here we consider the limiting case.

For such a polygon, the angle of the inward-pointing contact normal of edge n ($n \geq 3$) is $\eta = n\pi/k + \pi/2$. As $d \to \infty$, $\epsilon \to 0$, the angle ν from vertex n ($n \geq 3$) to the center of friction approaches $(n+k-1)\pi/k$. The required friction angle for a force to be applied through the center of friction from edge n is given by $\nu - \eta$ and therefore approaches $\pi/2 - \pi/k$ as $d \to \infty$, $\epsilon \to 0$. At any friction angle $\alpha < \pi/2 - \pi/k$, it is possible to choose d large enough and ϵ small enough that a pure force cannot be applied through edge n. Only edges 1 and 2 can apply pure forces. The positive span of these forces is confined to an open half-plane for any friction angle less than $\pi/2 - \pi/k$, and the slider is not small-time locally controllable. For any friction angle $\alpha \geq \pi/2 - \pi/k$, all edges can apply pure forces, and the slider is small-time locally controllable.

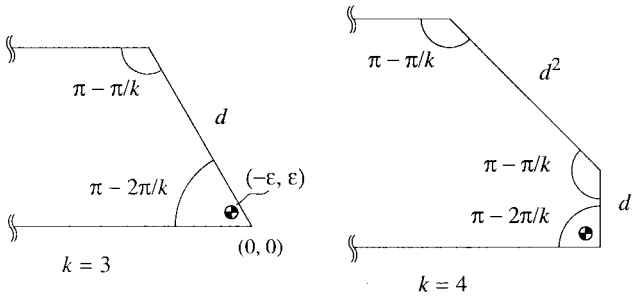

Fig. 16. As $d \to \infty$ and $\epsilon \to 0$, these polygons require the worst-case friction coefficient for small-time local controllability for k-gons (Section VI-B).

If we try to design a k-gon which is not small-time locally controllable with a friction angle greater than or equal to $\pi/2 - \pi/k$, we find that the polygon cannot be closed with only k edges while keeping pure forces confined to a half-plane. This fact is easily demonstrated by the following construction: choose the center of friction as the origin, and assume that pure forces can be applied from edges in the angle range $[\pi/2, 3\pi/2]$ relative to the origin (a half-plane of pure forces). Let $\alpha = \pi/2 - \pi/k$, and define the *edge at angle* β to be the edge of the polygon intersected by a ray from the origin at angle β. Then the requirement that no pure force can be applied from edges in the angle range $(-\pi/2, \pi/2)$ (the right half-plane) constrains the inward pointing contact normal η of the edges at angle $\beta \in (-\pi/2, \pi/2)$ to be outside the range $[\pi + \beta - \alpha, \pi + \beta + \alpha]$. A simple geometric argument shows that the slider cannot be closed by k edges while satisfying this constraint. The sliders described above are designed so as friction increases from zero, pure forces remain confined to a half-plane until friction has been increased so high that, simultaneously, pure forces can be applied from all edges.

C. Theorem 3

To investigate the limiting behavior, we drop the polygonal constraint and allow the slider to be any closed convex curve. This curve can be approximated arbitrarily closely by a polygon.

The problem is: given a friction angle α, find the slider that:

1) is marginally small-time locally controllable;
2) minimizes the ratio r of the radius ra of the circumscribed circle to the radius a of the inscribed circle.

This is equivalent to maximizing the friction coefficient necessary for small-time local controllability for a slider with ratio r. Without loss of generality, assume $a = 1$.

The solutions for several different values of r are shown in Fig. 17. Each slider consists of a circular arc, two spiral curves, and two line segments connecting the circular arc to the spiral curves. The circular arc is centered at the origin (the center of friction), has unit radius, and sweeps the angle from $-\pi/2 + \alpha$ to $\pi/2 - \alpha$. The two line segments are tangent to the ends of the arc and connect to $(0, \sec\alpha)$ and $(0, -\sec\alpha)$. The arc and line segments provide pure forces which positively span a half-plane. From there, the curve spirals away from the center of friction such that the tangent of the curve at every point is at an angle $\pi/2 + \alpha$ to the line connecting the curve

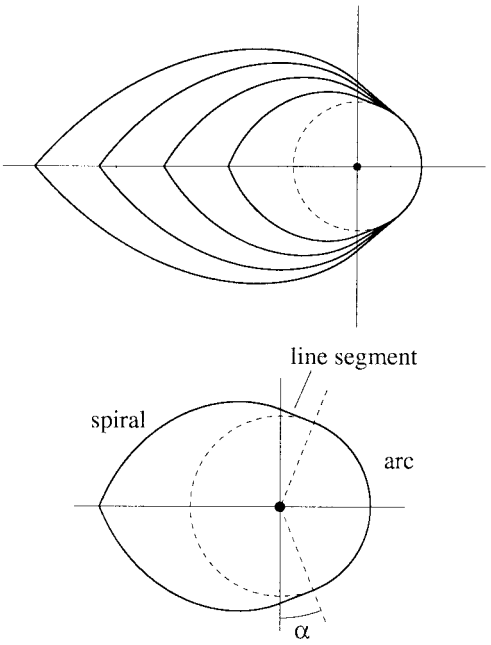

Fig. 17. Examples of sliders that maximize the required friction coefficient for small-time local controllability for $r = 2, 3, 4, 5$. The pieces of the slider are shown for $r = 2$.

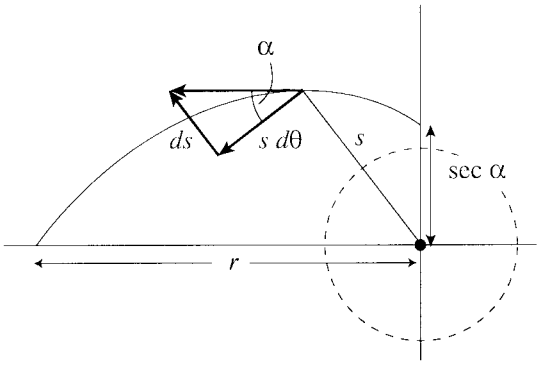

Fig. 18. Constructing the spiral segment.

to the center of friction. Thus, along the spiral segments, only boundary friction forces pass through the center of friction.

To find the top spiral, we solve the differential equation

$$ds = s\, d\theta \tan \alpha$$

where (s, θ) is the polar representation of the spiral (Fig. 18). Rearranging

$$\frac{ds}{s} = d\theta \tan \alpha$$

and integrating, we get

$$\ln s - \ln s_0 = (\theta - \theta_0) \tan \alpha$$

where (s_0, θ_0) is the start point of the spiral. Exponentiating and rearranging, we get

$$s = s_0 e^{(\theta - \theta_0) \tan \alpha}.$$

This is known as a *logarithmic* or *equiangular* spiral. Plugging in $s_0 = \sec \alpha$, $\theta_0 = \pi/2$, and the end angle $\theta = \pi$, we calculate r

$$r = \sec(\alpha) e^{(\pi/2) \tan \alpha}.$$

This curve gives the smallest possible value of r while keeping pure forces on the boundary. Furthermore, the arc and line segments minimize the value of s_0 while confining pure forces to a half-plane. Therefore, this slider minimizes r for a given α; equivalently, this slider maximizes the required friction angle α and coefficient μ for a given r.

This slider is only marginally small-time locally controllable for the friction angle α. For any friction angle less than α, we can find a polygonal approximation to the slider that is not small-time locally controllable. In particular, we can choose a piecewise linear approximation to the spiral such that no pure forces can be applied through it.

VII. Conclusion

By considering the part's geometry, center of friction, and pushing friction coefficient, this paper has characterized parts that can be maneuvered along arbitrary paths by open-loop stable pushing. These results help further establish the theoretical scope of pushing as a manipulation primitive.

Acknowledgment

The author would like to thank M. Mason and K. Goldberg for interesting discussions on controllability and completeness in robot manipulation and the anonymous reviewers for their suggestions on making the paper more readable.

References

[1] J. K. Salisbury, "Whole arm manipulation," in *Int. Symp. Robot. Res.*, Santa Cruz, CA. Cambridge, MA: MIT Press, Aug. 1987.
[2] M. Mani and W. R. D. Wilson, "A programmable orienting system for flat parts," in *Proc. N. Amer. Manufact. Res. Inst. Conf. XIII*, 1985.
[3] R. C. Brost, "Automatic grasp planning in the presence of uncertainty," *Int. J. Robot. Res.*, vol. 7, no. 1, pp. 3–17, Feb. 1988.
[4] M. A. Peshkin and A. C. Sanderson, "Planning robotic manipulation strategies for workpieces that slide," *IEEE J. Robot. Automat.*, vol. 4, pp. 524–531, Oct. 1988.
[5] K. Y. Goldberg, "Orienting polygonal parts without sensors," *Algorithmica*, vol. 10, pp. 201–225, 1993.
[6] S. Akella, W. Huang, K. M. Lynch, and M. T. Mason, "Planar manipulation on a conveyor with a one joint robot," in *Proc. Int. Symp. Robot. Res.*, 1995, pp. 265–276.
[7] Y. Okawa and K. Yokoyama, "Control of a mobile robot for the push-a-box operation," in *IEEE Int. Conf. Robot. Automat.*, Nice, France, 1992, pp. 761–766.
[8] B. R. Donald, J. Jennings, and D. Rus, "Information invariants for cooperating autonomous mobile robots," in *International Symposium on Robotics Research.* Cambridge, MA: MIT Press, 1993.
[9] H. J. Sussmann, "Lie brackets, real analyticity and geometric control," in *Differential Geometric Control Theory*, R. W. Brockett, R. S. Millman, and H. J. Sussmann, Eds. New York: Birkhauser, 1983.
[10] K. M. Lynch and M. T. Mason, "Stable pushing: Mechanics, controllability, and planning," *Int. J. Robot. Res.*, vol. 15, no. 6, pp. 533–556, Dec. 1996.
[11] K. M. Lynch, "The mechanics of fine manipulation by pushing," in *IEEE Int. Conf. Robot. Automat.*, Nice, France, 1992, pp. 2269–2276.
[12] Z. Li and J. Canny, "Motion of two rigid bodies with rolling constraint," *IEEE Trans. Robot. Automat.*, vol. 6, pp. 62–72, Feb. 1990.
[13] B. Mishra, J. T. Schwartz, and M. Sharir, "On the existence and synthesis of multifinger positive grips," *Algorithmica*, vol. 2, no. 4, pp. 541–558, 1987.
[14] X. Markenscoff, L. Ni, and C. H. Papadimitriou, "The geometry of grasping," *Int. J. Robot. Res.*, vol. 9, no. 1, pp. 61–74, Feb. 1990.

[15] E. Rimon and J. W. Burdick, "New bounds on the number of frictionless fingers required to immobilize planar objects," *J. Robot. Syst.*, vol. 12, no. 6, pp. 433–451, 1995.
[16] A. F. van der Stappen, K. Y. Goldberg, and M. H. Overmars, "Geometric eccentricity and the complexity of manipulation plans," *Algorithmica*, to be published.
[17] M. T. Mason, "Mechanics and planning of manipulator pushing operations," *Int. J. Robot. Res.*, vol. 5, no. 3, pp. 53–71, Fall 1986.
[18] M. T. Mason and R. C. Brost, "Automatic grasp planning: An operation space approach," in *Sixth Symposium on Theory and Practice of Robots and Manipulators.* Cracow, Poland: Alma-Press, Sept. 1986, pp. 321–328.
[19] M. A. Peshkin and A. C. Sanderson, "The motion of a pushed, sliding workpiece," *IEEE J. Robot. Automat.*, vol. 4, pp. 569–598, Dec. 1988.
[20] S. Goyal, A. Ruina, and J. Papadopoulos, "Planar sliding with dry friction. Part 1. Limit surface and moment function," *Wear*, vol. 143, pp. 307–330, 1991.
[21] ———, "Planar sliding with dry friction. Part 2. Dynamics of motion," *Wear*, vol. 143, pp. 331–352, 1991.
[22] J. C. Alexander and J. H. Maddocks, "Bounds on the friction-dominated motion of a pushed object," *Int. J. Robot. Res.*, vol. 12, no. 3, pp. 231–248, 1993.
[23] J. Barraquand and J.-C. Latombe, "Nonholonomic multibody mobile robots: Controllability and motion planning in the presence of obstacles," *Algorithmica*, vol. 10, pp. 121–155, 1993.
[24] J.-P. Laumond, P. E. Jacobs, M. Taïx, and R. M. Murray, "A motion planner for nonholonomic mobile robots," *IEEE Trans. Robot. Automat.*, vol. 10, pp. 577–593, Oct. 1994.
[25] M. A. Erdmann, "On motion planning with uncertainty," M.S. thesis, Mass. Inst. Technol., Cambridge, Aug. 1984.
[26] ———, "On a representation of friction in configuration space," *Int. J. Robot. Res.*, vol. 13, no. 3, pp. 240–271, 1994.
[27] H. J. Sussmann, "A sufficient condition for local controllability," *SIAM J. Contr. Optim.*, vol. 16, no. 5, pp. 790–802, Sept. 1978.

Kevin M. Lynch (S'90–M'95) received the B.S.E. degree in electrical engineering from Princeton University, Princeton, NJ, in 1989 and the the Ph.D. degree in robotics from Carnegie Mellon University, Pittsburgh, PA, in 1996.

He then spent a year and a half as an NSF/STA Postdoctoral Fellow in the Biorobotics Division, Mechanical Engineering Laboratory, Tsukuba, Japan. He also taught at the University of Tsukuba. Since 1997, he has been an Assistant Professor and Brewer Chair with the Mechanical Engineering Department, Northwestern University, Evanston, IL, where he co-directs the Laboratory for Intelligent Mechanical Systems. His research interests include robotic manipulation, flexible automation, and motion planning and control of underactuated robotic systems.

Dr. Lynch is Program Co-Chair for the Fourth Workshop on the Algorithmic Foundations of Robotics in 2000.